Research Article | Vol. 8, No. 10 | 1 Oct 2017 | BIOMEDICAL OPTICS EXPRESS 4504
Biomedical Optics EXPRESS

Examination of *Drosophila* eye development with third harmonic generation microscopy

ABIRAMY KARUNENDIRAN,[1,2] RICHARD CISEK,[3,4] DANIELLE TOKARZ,[5] VIRGINIJUS BARZDA,[3,4] AND BRYAN A. STEWART[1,2]

[1]*Department of Biology, University of Toronto Mississauga, 3359 Mississauga Road, Mississauga, Ontario L5L 1C6, Canada*
[2]*Department of Cell and Systems Biology, University of Toronto, 25 Harbord St, Toronto, Ontario M5S 3G5, Canada*
[3]*Department of Chemical and Physical Sciences, University of Toronto Mississauga, 3359 Mississauga Road, Mississauga, Ontario L5L 1C6, Canada*
[4]*Department of Physics and Institute for Optical Sciences, University of Toronto, 60 St. George Street, Toronto, Ontario M5S 1A7, Canada*
[5]*Princess Margaret Cancer Centre, University Health Network, 101 College Street, Toronto, Ontario M5G 1L7, Canada*

Abstract: Third harmonic generation (THG) microscopy can exploit endogenous harmonophores such as pigment macromolecules for enhanced image contrast, and therefore can be used without exogenous contrast agents. Previous studies have established that carotenoid compounds are ideal harmonophores for THG microscopy; we therefore sought to determine whether THG from endogenous carotenoid-derived compounds, such as retinal in photoreceptor cells, could serve as a new label-free method for developmental studies. Here we study the development of the pupal eye in *Drosophila melanogaster* and determine the localization of rhodopsin using THG microscopy technique. Additionally, by altering the chromophore or the opsin protein we were able to detect changes in both the retinal distribution morphology and in THG intensity age-dependent profiles. These results demonstrate that THG microscopy can be used to detect altered photoreceptor development and may be useful in clinically relevant conditions associated with photoreceptor degeneration.

OCIS codes: (000.1430) Biology and medicine; (190.4160) Multiharmonic generation; (190.1900) Diagnostic applications of nonlinear optics

References and links

1. R. W. Boyd, *Nonlinear Optics* (Amsterdam: Academic Press, 2008).
2. T. Y. F. Tsang, "Optical third-harmonic generation at interfaces," Phys. Rev. A **52**(5), 4116–4125 (1995).
3. A. F. Garito and K. Y. Wong, "Nonlinear optical processes in organic and polymer structures," Polym. J. **19**(1), 51 (1987).
4. J. R. Heflin, K. Y. Wong, O. Zamani-Khamiri, and A. F. Garito, "Nonlinear optical properties of linear chains and electron-correlation effects," Phys. Rev. B Condens. Matter **38**(2), 1573–1576 (1988).
5. R. Carriles, D. N. Schafer, K. E. Sheetz, J. J. Field, R. Cisek, V. Barzda, A. W. Sylvester, and J. A. Squier, "Invited review article: Imaging techniques for harmonic and multiphoton absorption fluorescence microscopy," Rev. Sci. Instrum. **80**(8), 081101 (2009).
6. E. A. Gibson, O. Masihzadeh, T. C. Lei, D. A. Ammar, and M. Y. Kahook, "Multiphoton microscopy for ophthalmic imaging," J. Ophthalmol. **2011**, 870879 (2011).
7. D. Tokarz, R. Cisek, M. Garbaczewska, D. Sandkuijl, X. Qiu, B. Stewart, J. D. Levine, U. Fekl, and V. Barzda, "Carotenoid based bio-compatible labels for third harmonic generation microscopy," Phys. Chem. Chem. Phys. **14**(30), 10653–10661 (2012).
8. R. L. Cagan and D. F. Ready, "The emergence of order in the Drosophila pupal retina," Dev. Biol. **136**(2), 346–362 (1989).
9. D. F. Ready, "A Multifaceted Approach to Neural Development," Trends Neurosci. **12**(3), 102–110 (1989).
10. T. Wang and C. Montell, "Phototransduction and retinal degeneration in Drosophila," Pflugers Arch. **454**(5), 821–847 (2007).
11. J. P. Kumar, "Building an ommatidium one cell at a time," Dev. Dyn. **241**(1), 136–149 (2012).

#295793 https://doi.org/10.1364/BOE.8.004504
Journal © 2017 Received 12 May 2017; revised 28 Jul 2017; accepted 5 Sep 2017; published 14 Sep 2017

Biomedical Optics EXPRESS

12. J. P. Kumar and D. F. Ready, "Rhodopsin plays an essential structural role in Drosophila photoreceptor Development," Development **121**(12), 4359–4370 (1995).
13. T. Wang, Y. Jiao, and C. Montell, "Dissection of the pathway required for generation of vitamin A and for Drosophila phototransduction," J. Cell Biol. **177**(2), 305–316 (2007).
14. C. Montell, "Drosophila visual transduction," Trends Neurosci. **35**(6), 356–363 (2012).
15. A. Major, D. Sandkuijl, and V. Barzda, "Efficient frequency doubling of a femtosecond Yb:KGW laser in a BiB3O6 crystal," Opt. Express **17**(14), 12039–12042 (2009).
16. C. A. Schneider, W. S. Rasband, and K. W. Eliceiri, "NIH Image to ImageJ: 25 years of image analysis," Nat. Methods **9**(7), 671–675 (2012).
17. T. Washburn and J. E. O'Tousa, "Molecular defects in drosophila rhodopsin mutants," J. Biol. Chem. **264**(26), 15464–15466 (1989).
18. S.C.R. Elgin, D.W. Miller, "Mass rearing of flies and mass production and harvesting embryos," (1978)
19. W. A. Harris, D. F. Ready, E. D. Lipson, A. J. Hudspeth, and W. S. Stark, "Vitamin A deprivation and Drosophila photopigments," Nature **266**(5603), 648–650 (1977).
20. D. Tokarz, R. Cisek, N. Prent, U. Fekl, and V. Barzda, "Measuring the molecular second hyperpolarizability in absorptive solutions by the third harmonic generation ratio technique," Anal. Chim. Acta **755**, 86–92 (2012).
21. S. W. Chu, I. H. Chen, T. M. Liu, P. C. Chen, C. K. Sun, and B. L. Lin, "Multimodal nonlinear spectral microscopy based on a femtosecond Cr:forsterite laser," Opt. Lett. **26**(23), 1909–1911 (2001).
22. F. J. Kao, "The Use of Optical Parametric Oscillator for Harmonic Generation and Two-Photon UV Fluorescence Microscopy," Microsc. Res. Tech. **63**(3), 175–181 (2004).
23. J. E. Treisman, "Retinal differentiation in Drosophila," Wiley Interdiscip. Rev. Dev. Biol. **2**(4), 545–557 (2013).
24. T. Washburn and J. E. O'Tousa, "Molecular defects in Drosophila rhodopsin mutants," J. Biol. Chem. **264**(26), 15464–15466 (1989).

1. Introduction

Third harmonic generation (THG) microscopy is a nonlinear optical imaging modality that can be used to reveal structural information in a biological system. A unique characteristic of this microscopy is that THG is observed at an interface between two media of different refractive indices and third-order nonlinear susceptibilities [1, 2]. This property provides the advantage of imaging multi-membranous structures at various focal depths. It was also found that THG signals are enhanced by molecules with large third-order nonlinear optical properties, termed harmonophores that contain long conjugated carbon chains [3, 4]. Therefore, samples containing such molecules can be imaged without altering the system by adding exogenous contrast agents. Another advantage of THG microscopy is that bleach free imaging can be performed [5–7], since light absorption does not have to occur during the coherent THG process, in contrast to fluorescence techniques. Carotenoid molecules are particularly suitable for THG, as shown in a previous study where carotenoid-liposomes were used to label drosophila Schneider 2 cells as well as *Drosophila melanogaster* larvae myocytes [7], where photobleaching free conditions were demonstrated by limiting the laser powers to <1 nJ with 1028 nm excitation.

We therefore sought to determine whether THG from endogenous carotenoid-derived compounds, such as retinal in photoreceptors, could serve as a platform to develop THG microscopy for developmental studies. Here, we used the compound eye of *Drosophila melanogaster* as a model system because of its well-known anatomy, developmental profile, and the availability of genetic tools. The *Drosophila* eye contains 750-800 ommatidia, a cluster of photoreceptor cells surrounded by support and pigment cells, each housing photoreceptor neurons that utilize the visual pigment rhodopsin, a G-protein coupled receptor for photo-transduction [8–11]. Rhodopsin is comprised of two subunits: a seven transmembrane protein called opsin, which is attached to a chromophore called retinaldehyde (retinal) via a Schiff-base linkage on the lysine residue in the seventh transmembrane domain [10]. The major opsin subunit (Rh1) is encoded by the *ninaE* gene and the chromophore is synthesized from vitamin A [12, 13]. High concentration of rhodopsin was found to be embedded within a specialized structure of the photoreceptor called rhabdomeres, which are a series of membrane folds that extend the entire length of the ommatidium [14]. It was previously found that the absence of either the protein subunit or the chromophore led to retinal degeneration [10, 12, 13].

Biomedical Optics EXPRESS

In this study, we investigated pupal retinal development using THG microscopic imaging. This was done by observing changes in pigment cell and photoreceptor structure at various pupal ages as well as by comparing the THG intensity localized in different regions of the retina. In a first series of experiments, we were able to show that THG microscopy would be an effective tool for monitoring normal ommatidial development, yielding both qualitative and quantitative results. In a second series of experiments, we used dietary restrictions of vitamin A or genetic alleles of the *ninaE* gene, which perturb rhodopsin synthesis or expression, to probe the origin of the THG signal and the consequences of such manipulations. In both cases, we observed changes in the organization and intensity of the THG signal. Our results demonstrate that THG microscopy can be used to observe ommatidial development and detect disruptions at a very early developmental stage. Therefore, THG microscopy can potentially monitor the development of the retina as well as aid in the detection of retinal degeneration, particularly syndromes linked to mutations of human rhodopsin.

2. Materials and methods

2.1 Nonlinear optical microscope

All imaging was performed using a custom-built, nonlinear microscope. The details of the laser system and the microscope setup are described elsewhere [5]. Briefly, the laser used for the microscope was based on a ytterbium-doped potassium gadolinium tungstate ($Yb:KGd(WO_4)_2$) crystal providing 430 fs duration pulses at 1028 nm wavelength with a pulse repetition of 14.3 MHz [15]. The average laser power at the sample was 15mW. An ultrafast-laser is used to satisfy the very high peak power requirement for harmonic generation, while keeping the average power low to avoid tissue damage.

The THG microscope setup is similar to a confocal microscope. Laser scanning is achieved via galvanometric scanning mirrors (SC2000 controller with two MiniSax amplifiers and VM1000 galvonometers, GSI Lumonics Inc), and operate at a maximum speed of 10 frames per second for a 128 × 128 pixel frame. The laser is focused on the sample via a microscope objective (20X Plan Apochromat, 0.75 NA, Zeiss). The THG signal is collected in the forward direction by a custom 0.8 NA collection objective. The signal is subsequently filtered by a bandpass filter (F10-340, CVI Melles Griot) and detected by a photomultiplier tube (H7421-40, Hamamatsu) set to single-photon counting mode, for efficient collection of the low intensity THG signal produced by the biological samples.

2.2 Imaging and analysis

For imaging, the sample was placed on a translation stage which moves laterally (x, y) as well as axially along the beam (z) direction, and was controlled using custom software in LabVIEW (National Instruments Corporation, Austin, TX). The THG response was obtained at a pulse energy of <1 nJ. All images shown have either a 40 x 40 μm or 30 x 30 μm area, and were imaged with similar laser powers, while THG intensities are the sum of photon counts in 100 frames. Image analysis was performed using ImageJ software (NIH, Bethesda, Maryland [16]). A region of interest was selected and a histogram of the photon counts for each pixel was created. The histogram was subsequently fitted with a single Gaussian function (OriginLab, Northampton, MA) to find the average signal for that region. Image intensities were normalized from day to day via standardizing to a measurement of 2 μm polystyrene beads (Duke Scientific Corporation) taken before each scan.

2.3 Drosophila rearing and strains

All flies were grown at 20°C on Bloomington standard cornmeal medium. Under our laboratory conditions, pupal development (pd) lasts approximately 150 hours. The pupal stages and the corresponding retinal development have been defined previously [8]. White

Biomedical Optics EXPRESS

pre-pupa on the sides of the vial were marked so that their development could be accurately recorded. Pupae where examined at 48, 72, 96 and 120 hours, corresponding to 32, 48, 64, and 80% of pupal development.

The w^{1118} strain was used as a control so that eye colour pigments usually found in the secondary and tertiary pigments cells would not interfere with the generation of THG signal. In addition, the following alleles of the *ninaE* gene were used: $ninaE^{1}$, $ninaE^{7}$, $ninaE^{8}$, which were obtained from the Bloomington Stock Center (Bloomington, Indiana University).

The *ninaE* gene encodes the opsin protein, which together with retinal, forms rhodopsin. Mutations in the *ninaE* gene were therefore analyzed. The $ninaE^{1}$ gene is a loss of function null allele that carries a nonsense mutation on the sixth transmembrane domain (Gln(251) nonsense), creating a premature stop codon. This strain produces essentially no wild-type rhodopsin [17]. In addition, two hypomorphic alleles, $ninaE^{7}$ and $ninaE^{8}$ were analyzed, both of which have reduced expression of opsin. Both $ninaE^{7}$ and $ninaE^{8}$ exhibit wild-type levels of the *ninaE* mRNA transcript, but have reduced protein levels compared to wild-type. The reduced rhodopsin levels are a result of missense mutations that cause changes in the amino acid sequence; $ninaE^{7}$ has a single mutation on the third transmembrane domain (Gly128Arg) whereas $ninaE^{8}$ has three mutations on the sixth transmembrane domain (Thr283Met, Trp289Arg and Cys297Ser).

In order to investigate the changes in THG signal with reduced retinal chromophore, w^{1118} flies were raised on vitamin A deficient media, which was adapted from [18]. This media contained (per L): 230 mL grape juice, 270 mL water, 40 g sucrose, 11 g Bacto-agar, 10 g yeast. 10 mL NaOH, and 2 mL of propionic acid. Adult flies were transferred into vials containing this media for one day to lay eggs. The adults were then removed and the larvae were allowed to grow and pupate. Lack of vitamin A did not affect the number of eggs laid or larval viability [18]. For the entire duration, the vials were maintained in a high humidity environment, since this medium dries out quicker than the standard medium.

2.4 Tissue dissection and sample preparation

When pupae had reached the appropriate developmental time, they were collected with small forceps and pinned down onto a Sylgard-filled Petri dish. The pupa was submerged in phosphate buffered saline (PBS) before the operculum of the pupal case was removed. With the pupa remaining in the case, the vitelline membrane and developing cuticle was pierced and cut in the sagittal plane with scissors. The brain with the attached retinas was extracted using a 20 µL pipettor and then placed in a watch glass containing 4% formaldehyde in PBS for 20 minutes. After washing the tissue with PBS, the retinas were removed from the optic lobes of the brain using dissection needles. The retinas were placed on a No. 1, 24 × 50 mm coverslip in a drop of PBS. A second No. 1, 24 × 24 mm coverslip was placed on top of the tissue, using small pieces of Parafilm as spacers between the two coverslips and sealed with nail polish to prevent drying.

3. Results

3.1 Nonlinear optical properties of developing Drosophila retinas

Pupal retinas from various developmental stages were imaged with THG microscopy. Z-stacks of images were collected by moving the focal plane of the laser through the tissue in 1 µm increments, for a total depth of approximately 30 µm. A schematic of a single ommatidium is given for reference (Fig. 1(A)).

Figure 1(A) presents a schematic of the ommatidium, indicating three levels of interest (A1-A3), while Fig. 1(B) shows typical THG images of the three levels at different pupal development (%) stages. The ommatidium top layer has bristle cells and the top of the secondary pigment cells (Fig. 1(A1) and 1(B1-4)). The pigment cell layer, which is 3-4 µm below the top layer, contains the pigment cells as well as the base of the bristle structure (Fig.

Biomedical Optics EXPRESS

1(A2) and 1(B5-8)), while the rhabdomere layer (A3 and B9-12), has the developing rhabdomeres and lower portion of the pigment cells. The hexagonal arrangement of pigment cells in a typical ommatidium can already be observed in 32% pd retinas (Fig. 1(B1) and 1(B5)). The bristle cells begin to be observed at 48% pd (indicated by arrowhead in B2), and have intense signal starting at 64% pd (Fig. 1(B3)). The pigment cells are clearly defined at 48% pd (Fig. 1(B6)). Several changes in the ommatidial structure can be observed in THG images at 64% pd. Approximately 8-10 µm below the pigment cell layer, bright star-shaped structures are observed in an array-like pattern where each structure is surrounded by low-intensity hexagonal regions (Fig. 1(B11)-1(B12)). The low intensity hexagonal regions (arrow i in Fig. 1(B11)) are attributed to the lower portion of pigment cells, while the star-shaped structures (arrow ii in B11), located at the center of the hexagonal shapes, are attributed to developing rhabdomeres and can be observed for approximately 10µm in depth. Similar morphology in the pigment cells and bristle groups were observed in 80% pd retinas (Fig. 1(B4), 1(B8) and 1(B12)). THG signal generated by the rhabdomeres in 80% pd (Fig. 1(B12)) exhibited a star-shape at closer contact, representative of rhabdomere maturation, where the membrane projections elongate towards the center of the ommatidium [10, 14]. These data show for the first time the potential utility of THG microscopy for the analysis of eye development in unstained tissue.

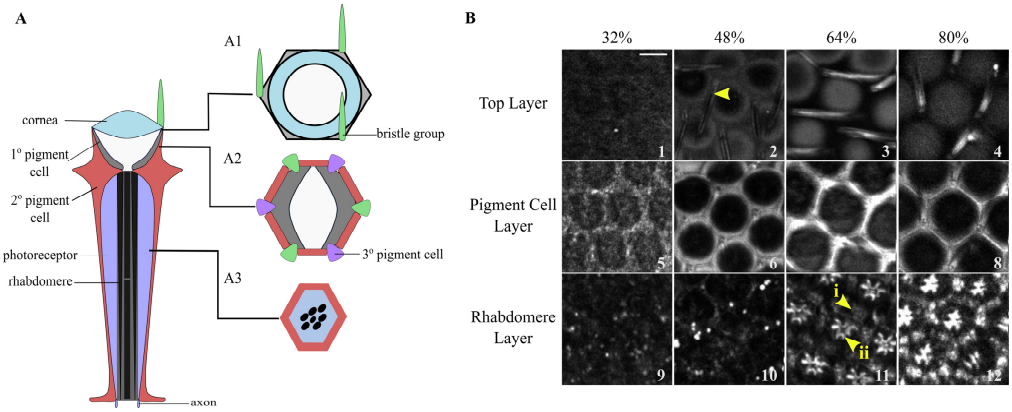

Fig. 1. THG microscopy images of the developing retina during the pupal stage along with a schematic of an ommatidium. (A) A simplified schematic of a single ommatidium showing three focal depths of interest. (B) THG images at the three focal depths of interest (rows) at four stages of pupal development (columns, %). Images are normalized to excitation energy. The scale bar represents 10 µm.

Following the morphological characterization of THG signals arising from *Drosophila* retina, the signal intensity was quantified for each pupal development stage. THG signal intensity localized in the pigment cells and in the rhabdomeres was quantified via manual selection of regions of interest, shown in yellow (Fig. 2(A) and 2(B)), and at each developmental stage the average THG intensity was extracted using ImageJ. For rhabdomeres in the 32% and 48% pd retinas, THG intensity values were measured from images collected 10 µm below the lattice layer, at the focal plane where the rhabdomeres were observed in later developmental stages.

The THG signal intensity from the pigment cells was found to steadily increase from 32 to 64% pd, but then the intensity decreased at 80% pd. THG intensities in the rhabdomeres were initially low but increased steadily throughout development. The difference in THG intensities between the pigment cells and rhabdomeres was significantly larger in 48% pd retinas (2.9x) when compared to 32% pd pupas (1.8x), where both differences were significant (two-tailed T-test, $P < 0.001$). The difference between the two cell types decreases in the 64% pd retinas to 1.4 times, due to the sharp increase in rhabdomere THG intensity (P

Biomedical Optics EXPRESS

< 0.001). In 80% pd retinas, the THG intensity in the rhabdomeres was found to be 1.8x times higher than that of the pigment cells (P < 0.001). The changes in THG intensity in the pigment cells and rhabdomeres could be due to changes in both the cellular structure of the ommatidium and in the transport of rhodopsin to the rhabdomeres.

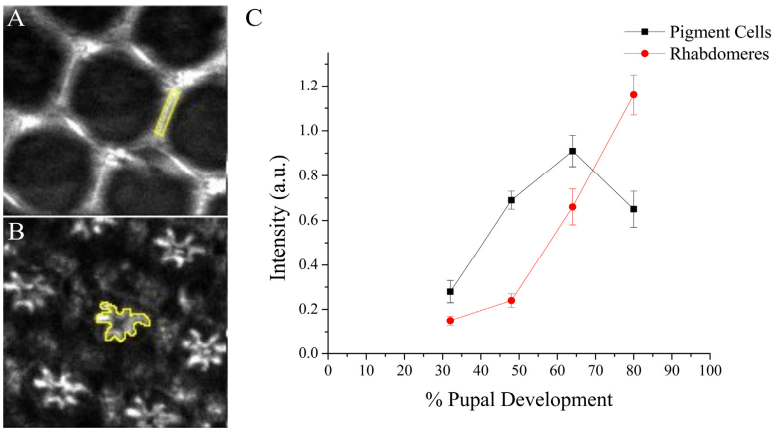

Fig. 2. A method to measure the localized THG intensity, and corresponding THG intensity-dependent curve for w^{1118} pupal retinas. The THG localized in either the pigment cells (A) or in the rhabdomeres (B) were measured. (C) The resulting THG intensity graph shows changes in THG intensities of the pigment cells and the rhabdomeres during pupal development. Highlighted regions in (A) and (B) are used to calculate the THG intensities. Error bars represent standard error of the average THG intensity measured from 11 pupae.

3.2 Effects of vitamin A deficiency on THG signal from pupal retinas

In order to determine if the THG signals are dependent on the retinal-based photopigments, flies were reared on vitamin A deficient media. Such flies should have reduced availability for the chemical precursor to synthesize retinal. Thus, any changes in THG signal from retinas of this treatment compared to flies raised in normal media can help determine whether the THG signal is originating from retinal, membrane interfaces or both [13, 19]. Figure 3 presents THG images of the top, pigment cell and rhabdomere layers (see Fig. 1(A)) for different pupal development stages.

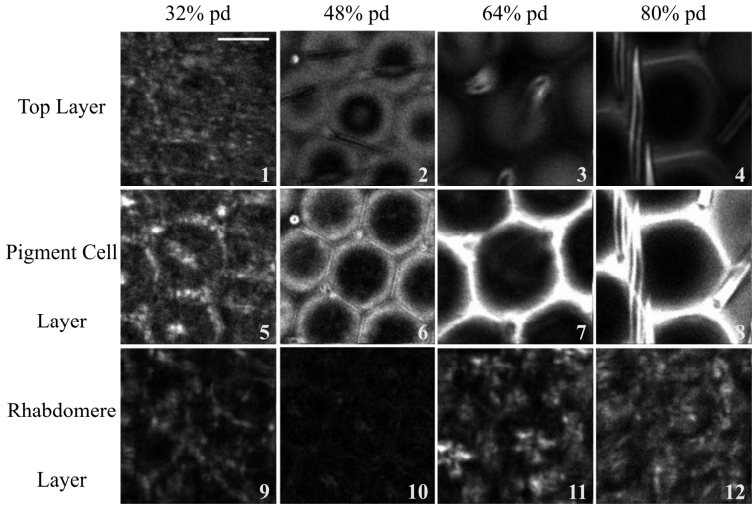

Fig. 3. THG microscopy images of the vitamin A deficient developing retina during the pupal stage. Three focal depths of interest (see Fig. 1(A)) are shown in rows, and pupal development stages are shown in columns. The scale bar represents 10 µm.

Biomedical Optics EXPRESS

In the vitamin A deficient mutant, the bristle groups are observed to develop in a similar way to the flies reared in normal media (compare Fig. 3 panels 1-4 to Fig. 1(B1)-1(B4)). Similarly, the pigment cells (panels 5-8) also appear to develop similarly to the normal flies, suggesting that THG signal from pigment cells does not depend on retinal. Rhabdomeres (arrowhead in panel 11) along with the lower region of the pigment cells were observed at 64% pd, but with lower THG intensity compared to flies reared on the normal diet. The most prevalent changes can be observed in the rhabdomeres and photoreceptors in 80% pd (compare Fig. 3, panel 12 to Fig. 1 panel B12) where substantial structural changes are observed, showing low intensity disorganized structures in the vitamin A deficient flies as compared with star shapes in the control.

As with flies reared on normal media, the THG signal intensities were quantified for the pigment cells and the rhabdomeres in pupae raised on vitamin A deficient media (Fig. 4(A) and 4(B)). The average THG intensity measured in 32% pd vitamin A deficient pigment cells was very similar to the value found in the control (two tailed T test, $P < 0.001$). Only a slight increase in the intensity occurred between 32% and 48% pd, much lower compared to the control ($P < 0.001$), as expected if THG is generated by mostly retinal. However, a sharp intensity increase of 4 times occurred in the pigment cells between 48% and 64% pd, resulting in a 1.3x higher intensity of the vitamin A deficient fly at 64% pd than the fly reared on cornmeal ($P<0.0001$). Furthermore, the intensity did not decline at 80% as the control did, which was not as predicted.

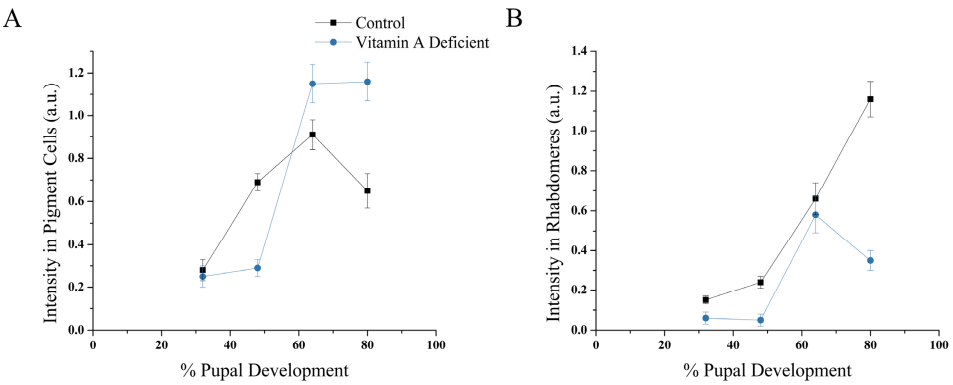

Fig. 4. THG intensity curves localized in pigment cells and in the rhabdomeres in vitamin A deficient pupae in comparison to cornmeal reared w^{1118}. (A) Comparison of the THG intensities in pigment cells. (B) Comparison of the THG intensities in the rhabdomeres.

A different trend was observed with the rhabdomeres from flies raised on vitamin A deficient media (Fig. 4(B)). The average THG intensities measured in all four developmental stages were found to be lower than the intensity obtained for pupae raised on normal media ($P < 0.001$ for all four stages). No intensity change was observed between 32% and 48% pd, which did not match the trend of the normal flies. Then an increase in THG intensity of 11 times was observed between 48% and 64% pd, which is attributed to the development of rhabdomere membranes. A decrease in the average intensity of 1.6 times was measured in 80% pd resulted in a difference of 3.3 times in intensity when compared to the control. This can be attributed to the degradation of the rhabdomeres observed in the THG intensity images of 80% pd retinas (Fig. 3).

The THG intensity curve at the rhabdomeres with vitamin A deficiency has a similar trend to the control curve from 32% to 64%, suggesting that rhabdomeres lacking the ability to produce retinal develop normally in the earlier stages. However, the intensities were lower than control at all four stages of pupal development, corresponding to the morphological changes detected in THG images during the latter stages. This suggests that reduced levels of

Biomedical Optics EXPRESS

retinal causes the decrease in THG intensity. The intensity localized at the pigment cells of vitamin A deficient retina was found to sharply increase between 48% and 64% pd, and obtain a higher intensity than the w^{1118}, which is not expected. This may indicate that vitamin A deficiency induces a change in the morphology of the pigment cells, resulting in this sudden increase in THG intensity within the pigment cells but further work is required to establish this assertion.

3.3 Manipulation of opsin protein – analysis of ninaE *alleles*

As a second method to manipulate the visual photopigments, we took advantage of mutants of the *ninaE* gene. Similar to the vitamin A deficient retina, no notable changes in the ommatidial structure was detected in 32% and 48% pd pupa, where hexagonal lattice arrangement developed at the same rate as the control (data not shown). Structural changes were noted in 64% and 80% pd retinas (Fig. 5). The pigment cells and bristle structures were observed to be similar to w^{1118} for both 64% (Fig. 5 Panels 1, 5 and 9) and 80% pd (Fig. 5 Panels 3, 7 and 11) and are unaffected by the reduced levels of Rh1. However the rhabdomeres were not structurally similar to the control in 64% pd (Fig. 5 panels 2, 6 and 10). Further, the rhabdomeres are not as visible in 80% pd (Fig. 5 panels 4, 8, 12). These results indicate that rhabdomeres degradation started as early as 64% pd and become less structurally intact with pupal development. Morphological comparisons show that degradation of the rhabdomeres in the *ninaE* pupae occur at different rates, where $ninaE^{1}$ (Fig. 5 panel 2,4) and $ninaE^{8}$ (Fig. 5 panel 10, 12) rhabdomeres degrade faster than $ninaE_{7}$ rhabdomeres (Fig. 5, panel 6, 8).

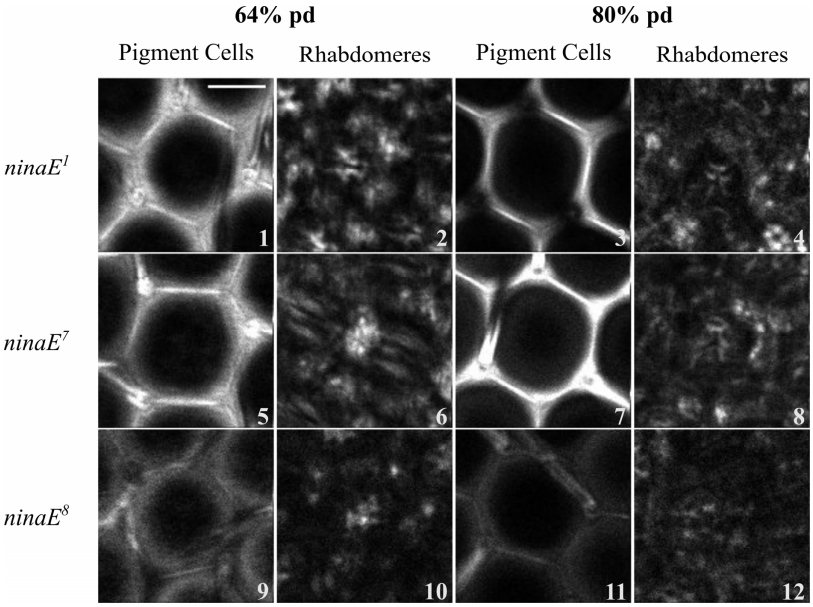

Fig. 5. THG images of pigment cells and rhabdomeres during the latter stages in each *ninaE* mutant. For each genotype, THG images of the pigment cells and rhabdomeres are shown for 64 and 80% pd. Scale bar represents 10 µm.

The THG intensities for each *ninaE* mutant were quantified and compared to w^{1118} (Fig. 6). The THG intensities measured in 32% pd retinas for each mutant was found to be similar to that of the control in the pigment cells (ANOVA, $P < 0.001$). A significant increase in the intensity measured in the pigment cells (with the exception of $ninaE^{8}$) was observed in 48% pd. This resulted in the $ninaE^{1}$ and $ninaE^{7}$ THG intensities to be higher than the control at that stage, where the highest value was measured in $ninaE^{1}$ pigment cells. However, a decrease in the THG intensity was seen in all of the *ninaE* mutants at 64% pd, where their values were

Biomedical Optics EXPRESS

found to be similar to, or lower than the control ($P < 0.001$). A similar trend was seen in 80% pd, where *ninaE*^{1} was similar to the control, *ninaE*^{7} was higher than the control and *ninaE*^{8} was lower.

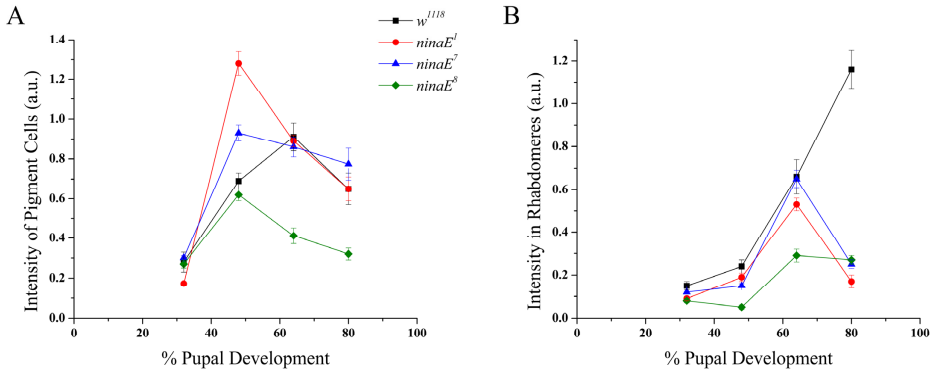

Fig. 6. Comparison of THG intensities between *ninaE* mutants and the control pupal retinas. (A) THG intensities localized in the pigment cells of each mutant were shown to produce a different curve compared to the wild type. (B) THG intensities localized in the rhabdomeres in each mutant were found to have a similar curve as the wild type until 64% pd.

In general in *ninaE* mutants, the THG intensities of rhabdomeres followed the trend of the w^{1118} flies up to 68% pd, and then the intensities dramatically dropped at 80% pd (see Fig. 6). In the first two stages, the THG intensities measured in the rhabdomeres of each mutant was found to be lower than the control at each developmental stage (ANOVA, $P < 0.01$). Both *ninaE*^{1} and *ninaE*^{7} increased, similarly to the w^{1118}, however, *ninaE*^{8} is shown to decrease at 48% pd. At 68%, all three mutants increased THG intensity, with *ninaE*^{7}, which had the same intensity as the w^{1118}, while the other two mutants had lower intensities. The dramatic decrease in THG intensity at 80% pd showed a very different behavior than the w^{1118} which increased at that stage and may suggest that rhodopsin transport begins at 64% pd.

4. Discussion

Here we have demonstrated the potential of THG microscopy as a valuable imaging tool to detect changes in rhodopsin concentration and localization along with its effect on rhabdomere morphology in *Drosophila* retina. In this study we found that both carotenoids and cell structure contribute to THG signals arising from retinal tissues.

A Yb:KGW femtosecond laser is well-suited to rhabdomere imaging due to high nonlinear susceptibilities of carotenoids at 1028 nm wavelength [7, 20]. It should be, that THG signal occurs at a wavelength of 343 nm and requires specialized collection objective and UV enhanced detectors when imaged with Yb:KGW laser. A Cr:forsterite or an optical parametric oscillator based femtosecond laser could be used to shift the THG signal to the visible wavelength for imagining with regular commercial multiphoton excitation microscopes [21, 22]. The longer wavelengths provide higher penetration depth into a biological sample albeit with reduced spatial resolution of the microscope.

Our 3D analysis of the ommatidia showed structural changes due to maturation and the presence of *ninaE* mutations. THG images of the developing pupal retina revealed pigment cell and bristle group development in the earlier stages and the elongation of rhabdomere membranes in the latter stages, corresponding with previous findings [8, 23]. Pupa with either dietary restrictions or genetic alleles that reduce rhodopsin synthesis or expression were shown to have either slower development or degeneration of the rhabdomere membrane, indicating that the visual pigment rhodopsin augments THG signals found in the retina. Furthermore, quantitative analysis of the pupal retina shows changes in the THG intensity throughout development in both the pigment cells and rhabdomeres (Fig. 2). These changes

Biomedical Optics EXPRESS

can be explained using what is already known about rhodopsin synthesis and localization during pupal development. At the earlier stages of pupal development, synthesized retinal is mostly localized in the pigment cells [13]. During development the retinal is transported to the rhabdomeres. The intensity curve suggests that the change in THG intensity in the pigment cells and rhabdomeres is due to the transport of the chromophore, which is known to contain a conjugated carbon chain. The THG intensity curve in w^{1118} pupae suggest that retinal begins to be transported to the photoreceptors after 48% pd.

Although loss of the chromophore was shown to decrease THG intensities in the rhabdomeres (Fig. 4), the *ninaE* experiment indicates that decrease in chromophore binding due to changes in the opsin structure seems to have a more pronounced effect on the rhabdomere structure, causing a decrease in THG intensity (Fig. 6). This can be explained with what was previously found by Washburn et al. [24]. The mutation in $ninaE^{1}$ flies caused the loss of the sixth and seventh transmembrane domain, which consequentially resulted in the loss of the chromophore-binding site and reduced opsin levels. Similarly, $ninaE^{8}$ flies contain a point mutation that caused a less hydrophobic sixth transmembrane domain, and was suggested that rhodopsin to lose this domain along with the binding site. The mutation in $ninaE^{7}$ flies, on the other hand, only affects the third transmembrane domain. This along with the data from THG images in this paper suggests that mutations affecting the sixth and seventh transmembrane domain, and therefore affecting the chromophore binding site of rhodopsin caused faster degradation of the rhabdomeres. Both the *ninaE* mutations and the vitamin A deficiency study suggest that rhabdomere degeneration can be detected at 64% pd, which is an earlier stage than what was previously found [12], where confocal fluorescence microscopy was utilized to observe the localization of Rh1. This study suggests that THG microscopy can be used to gain new insight on retinal degeneration by tracking the movement and localization of carotenoids, a feature that is not present in the more readily available fluorescence microscopy. THG intensity profile differences between mutants with vitamin A deficiency and reduced levels of opsin suggest this technique can be potentially developed to identify different retinopathies. As this technology develops further, capturing harmonic signals with lower intensity light may allow for *in vivo* examination of altered retinal structure in diseases of the eye.

Funding

This work was supported by grants from the Natural Sciences and Engineering Research Council of Canada to BAS and VB.

Acknowledgements

Stocks obtained from the Bloomington Drosophila Stock Center (NIH P40OD018537) were used in this study.

Disclosures

The authors declare that there are no conflicts of interest related to this article.